

TG-FTIR, DSC, and Quantum-Chemical Studies on the Thermal Decomposition of Quaternary Ethylammonium Halides

Marlena Sawicka, Piotr Storoniak, Jerzy Błażejowski, and Janusz Rak*

Faculty of Chemistry, University of Gdańsk, Sobieskiego 18, 80-952 Gdańsk, Poland

Received: December 23, 2005; In Final Form: February 27, 2006

The thermal decomposition of quaternary ethylammonium chloride, bromide, and iodide has been studied using the experimental techniques of thermal gravimetry coupled to Fourier transform infrared spectroscopy (TG-FTIR) and differential scanning calorimetry (DSC) as well as the density functional theory (DFT) and MP2 quantum-chemical methods. These compounds decompose in a one-step process, and the almost perfect agreement between the experimental IR spectra and those predicted at the B3LYP/6-311G(d,p) level demonstrates for the first time that decomposition produces an equimolar mixture of triethylamine and a haloethane. The respective experimental enthalpies of dissociation of the chloride, bromide, and iodide are 158, 181, and 195 kJ/mol. These values correlate well with the calculated enthalpies of dissociation based on crystal lattice energies and quantum-chemical thermodynamic barriers. The experimental activation barriers were derived from the least-squares fit of the F1 kinetic model (first-order process) to thermogravimetric traces. These estimates are 184, 286, and 387 kJ/mol for chloride, bromide, and iodide, respectively, and agree well with the theoretical calculations. It has been demonstrated that the theoretical approach assumed in this work is capable of predicting the relevant characteristics of the thermal decomposition of solids with experimental accuracy. DFT methodology is recommended for the quantum-chemical part of the model: B3LYP for evaluating the thermodynamic barriers and MPW1K for assessing the activation characteristics. These quantum-chemical data then have to be combined with crystal lattice energies. The latter should be calculated using both electrostatic and repulsion–dispersion terms.

1. Introduction

The numerous attractive properties of the salts of quaternary nitrogen organic bases (SQNOBs) are justification enough for the on-going interest in this group of compounds and have led to their being applied in a variety of ways. Being effective surfactants, SQNOBs are some of the most potent antielectrostatic agents for synthetic polymers.¹ Since they display antifungal and antibacterial activity, they are common ingredients of timber preservatives.² Their biological activity has also rendered them useful in treatments for diabetes, cardiac arrhythmia, neurosis, and allergies.³ The role of SQNOBs in inactivating the HIV virus and in potentiating anticancer drugs has been reported recently.⁴ These substances are also widely used in the laboratory and industry as counterions in phase transfer catalysis (PCT), thus ensuring the selectivity of reactions, and the high yields and purity of their product(s).⁵ Furthermore, many SQNOBs behave like ionic crystals; consequently, they make excellent solvents for a wide range of reactions such as polymerization,⁶ olefin production via aldehyde reduction,⁷ epoxide formation,⁸ alkylation,⁹ hydrogenation,¹⁰ and the Friedel–Crafts¹¹ and Wittig¹² reactions. Finally, owing to their relatively simple thermal behavior, SQNOBs are convenient models for investigating the thermal decomposition of solids.^{13–15}

Much of the available knowledge on the thermal stability of solids is empirical. Therefore, the long-term goal of studying the decomposition of solids is to develop a theory explaining the thermal stability of different substances and enabling the

thermal behavior of untested compounds to be predicted. The most promising approach to this question seems to be the one that combines kinetic studies focusing on an accurate mathematical description of the experimental results with theoretical investigations attempting to relate the experimental data to processes occurring at the molecular level.¹⁶

As we have already mentioned, the attractive thermal properties of the salts of quaternary nitrogen organic bases make these compounds convenient systems for working out a theory linking the experimentally observed thermal behavior of solid substances with theoretical information on the molecular characteristics of individual ions and selected crystal structure characteristics. This is why our team has been investigating the thermal behavior of this class of compounds for some time now. Besides the halides of *N*-methylated heterocyclic amines¹⁷ and quaternary *N*-alkanaminium halides,^{13–15} we have studied primary, secondary, and tertiary *N*-alkanaminium ($[(C_nH_{2n+1})_pNH_{4-p}]X$, where $n = 1–4$, $p = 1–3$, and $X = Cl, Br, I$)^{13–15} and *N*-arylamminium halides,¹⁸ mainly with the aid of thermodynamic analyses. As our own thermochemical data and other experimental studies^{19,20} have suggested, these compounds decompose at elevated temperatures in quite a simple way. Thermal dissociation probably leads to two gaseous products: one of them is a free base, but the identity of the other species depends on the system being heated. Specifically, a hydrogen halide is likely to be produced from primary, secondary, and tertiary halides, and an alkyl halide is likely to be produced from quaternary salts.

Several thermodynamic and kinetic characteristics of these quaternary salts and amine hydrohalides have been derived from our thermoanalytical investigations so far: the enthalpies of

* To whom correspondence should be addressed. E-mail: janusz@raptor.chem.univ.gda.pl.

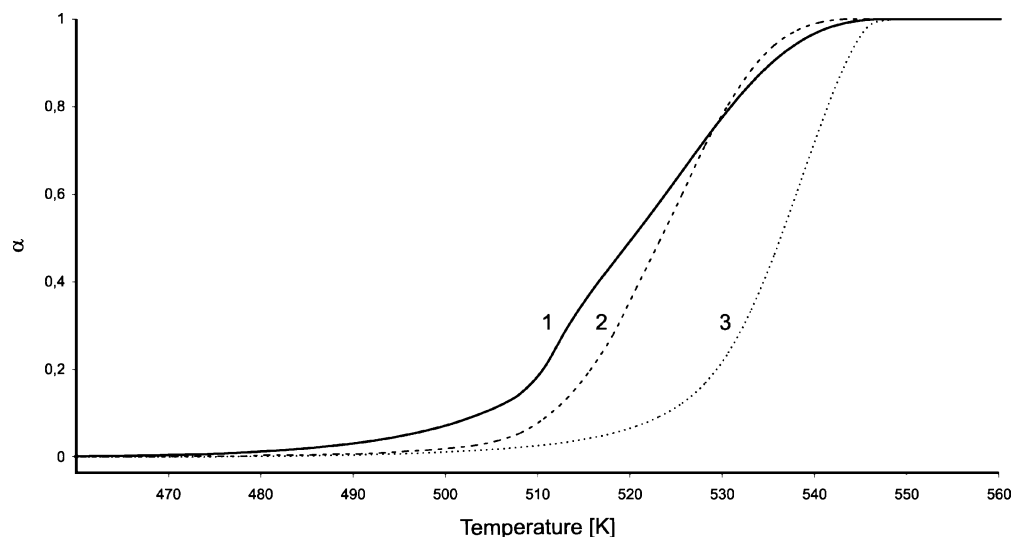


Figure 1. Thermodynamic traces recorded for decomposition of *N,N,N*-triethylethanammonium chloride (1), *N,N,N*-triethylethanammonium bromide (2), and *N,N,N*-triethylethanammonium iodide (3).

thermal dissociation, the enthalpies of formation, and the crystal lattice energy of these salts on the basis of thermogravimetric measurements,^{13–15} with the last-mentioned property using both the thermochemical cycle and the Kapustinskii–Yatsmirski method.^{21,22} As far as crystal energy is concerned, we should also mention a series of papers that our team has published on the direct estimation of the electrostatic part of the crystal lattice energy.^{23–27} Here, structural information from diffraction measurements, the charge distribution in a complex cation, usually calculated with a semiempirical or an *ab initio* quantum-chemical method, and Ewald's summation²⁸ were employed to evaluate the electrostatic energy.

Several kinetic models have been used to describe the kinetics of the volatilization of quaternary salts and amine hydrohalides. It was found, for instance, that the R1 (zero kinetic order) and R2 (contracting surface) reaction mechanisms were the most appropriate for describing the thermal dissociation kinetics of primary, secondary, and tertiary amine hydrohalides, whereas the F1 (first-order) model was suitable for analyzing the thermal degradation of quaternary salts.^{13–15} Besides these quantitative characteristics, a number of qualitative observations were also made: for example, the enthalpy of volatilization increased gradually with the increasing size of the alkanaminium cation, and the absolute enthalpy of formation increased while the lattice energy decreased with the number of alkyl groups in the amine molecule.^{13–15}

The thermal properties of quaternary ethylammonium halides (QEtA) have been the subject of several of our investigations: experimentally by thermogravimetry (TG)^{13–15,27,29} and also by semiempirical and *ab initio* methods.^{27,29} In the current study we applied several experimental techniques and theoretical methods to study the thermal behavior of QEtA.

This paper reports on the thermodynamics and kinetics of the thermal decomposition of the title compounds studied with the thermoanalytical techniques of thermogravimetry coupled to Fourier transform infrared spectroscopy (TG-FTIR) and differential scanning calorimetry (DSC). First, we compare the FTIR absorption spectra of the products formed during thermal decomposition with the theoretical ones. From this comparison we have been able to draw unequivocal conclusions regarding the mechanism of thermal decomposition. Second, we contrast the DSC measurements with the theoretical dissociation enthalpies calculated from the crystal lattice energies and correlated

ab initio models. Finally, we analyze the activation energies of the process in terms of the quantum-chemical barriers obtained for the assumed mechanism and the calculated crystal lattice energies. The very good correspondence between the enthalpies of activation obtained from the thermogravimetric curves and those modeled quantum mechanically suggest that quaternary ethylammonium halides decompose via a unimolecular process.

2. Methods

2.1. Experimental Procedures. All quaternary salts were purchased at the best available grades and then purified by recrystallization from methanol, ethanol, or a mixture of methanol with ethyl ether, as prescribed in the literature.^{30,31} The final purity of the compounds was checked by elemental analysis on a Carlo Erba Eager 200 instrument.

Dynamic thermogravimetric measurements (TG) were conducted on a Netzsch TG 209 thermobalance coupled to a Bruker IFS 66 FTIR spectrometer. Samples weighing 9–12 mg were placed in a platinum crucible and heated at (β) 2.5 K min⁻¹ in a dynamic argon atmosphere.

Differential scanning calorimetry measurements were carried out on a Netzsch DSC 204 instrument. Samples weighing 8–17 mg were placed in an aluminum crucible covered with a lid (with a pinhole) and heated at 2.0–5.0 K min⁻¹ in a dynamic Ar atmosphere. These experiments allow the enthalpies of dissociation ($\Delta_d H^\circ$) to be measured directly.

Enthalpies of dissociation were also estimated by fitting thermogravimetric traces (see Figure 1) to the following formula (van't Hoff equation):^{13–15}

$$\ln \alpha = -\frac{\Delta_d H^\circ}{2R} \frac{1}{T} + \frac{\Delta_d H^\circ}{2R} \frac{1}{T_d} \quad (1)$$

where α is the extent of the reaction; T_d is the temperature at which $\alpha = 1$; R is the gas constant.

Finally, the activation enthalpy of the decomposition process ($\Delta_a H^\circ$) was derived by fitting the TG curves to the general equation:

$$g(1 - \alpha) = \frac{Z}{\Phi} T \exp\left(\frac{\Delta_a H^\circ}{RT}\right) \quad (2)$$

where Z is the Arrhenius preexponential factor. $g(1 - \alpha)$ is the

integral form of the function describing the kinetic model assumed: zero kinetic order (R1), $g(1 - \alpha) = \alpha$; surface decomposition (R2), $g(1 - \alpha) = 1 - \ln(1 - \alpha)^{1/2}$; unimolecular decomposition (F1), $g(1 - \alpha) = -\ln(1 - \alpha)$.

Fitting was applied only to those parts of the TG curves corresponding to α in the ca. 0.2–0.9 range.

2.2. Computational Methods. The crystal lattice energy (E_c) was calculated by summing the electrostatic (E_{el}), dispersive (E_d), and repulsive (E_r) contributions:

$$E_c = E_{el} + E_d + E_r \quad (3)$$

E_{el} in eq 3 represents Coulombic interactions:

$$E_{el} = \frac{1}{2} \sum_i \sum_{j \neq i} \frac{Ne^2 Q_i Q_j}{4\pi\epsilon_0 R_{ij}} \quad (4)$$

while the sum of E_d and E_r is expressed by the Buckingham equation:³²

$$E_d + E_r = \frac{1}{2} \sum_i \sum_{j \neq i} \left[-\frac{D_i D_j}{R_{ij}^6} + B_i B_j \exp(-C_i C_j R_{ij}) \right] \quad (5)$$

In eqs 3–5 N is the Avogadro number; e is the elementary charge; ϵ_0 is the permittivity of free space; Q_i and Q_j are the relative partial charges at given atoms; D_i (D_j), B_i (B_j), and C_i (C_j) are their van der Waals atomic parameters; and R_{ij} is the distance between interacting centers (the summation extends over all pairwise interactions between each atom of a molecule chosen as a basic stoichiometric unit (denoted by “ i ”) and all atoms from its surroundings (denoted by “ j ”). The electrostatic part of the crystal lattice energy was calculated assuming a 1+ charge on tetraethylammonium cations (NEt_4^+) and a 1− charge on a halogen anion (X^-). The charges on particular atomic centers of the cations were derived from the fit to the electrostatic potential (MEP fit)³³ predicted at the density functional theory level. The atomic parameters necessary for calculating $E_d + E_r$ contributions for all but bromine and iodide atoms were taken from Filippini and Gavezzotti,³⁴ while those for Br and I were adopted from Goddard et al.³⁵ Crystal lattice energies were calculated using the structural data of tetraethylammonium chloride,³⁶ bromide,³⁷ and iodide³⁸ available in the literature.

The initial geometries of the stationary points on the potential energy surface of the dissociation reaction were localized using the computationally efficient semiempirical PM3 method.³⁹ These structures were further optimized at the density functional theory (DFT) with a Becke’s three-parameter hybrid functional (B3LYP)⁴⁰ and MP2 levels using the 6-311G(d,p) basis set.^{41,42} Since the stability of an ionic pair ($[\text{NEt}_4 \cdots \text{X}]$; see below) is necessary for estimating an activation barrier, the effect of basis set superposition error (BSSE) on the interaction energy was checked within these van der Waals complexes. The value of BSSE did not exceed 8 kJ/mol at the B3LYP/6-31G(d,p) level, whereas the interaction energy uncorrected for BSSE was 320–370 kJ/mol (see below). We therefore present our interaction energy results without counterpoise corrections.

The matrices of the second derivatives of the energy with respect to geometry (Hessians) were calculated to confirm that the final geometries were minima (all positive eigenvalues) or transition states (exactly one negative eigenvalue). To verify the correctness of the transition state (TS) structures, we visualized the normal mode corresponding to the imaginary frequency. Additionally, the intrinsic reaction path (IRC) was

followed at the B3LYP/6-311G(d,p) level, starting with the TS structure for tetraethylammonium chloride, bromide, and iodide, which confirmed that the located transition states were always linked to the relevant substrate and products.

The B3LYP method is known to underestimate reaction barriers.⁴³ For this reason, additional geometry optimizations were performed employing the MPW1K exchange-correlation functional, which was parametrized to reproduce barrier heights for chemical reactions.⁴³ The quantitative agreement between the MP2, B3LYP, and MPW1K predictions strengthens our conclusion.

Only the B3LYP method was employed to calculate harmonic vibrational frequencies and zero-point energies, which enabled selected thermodynamic characteristics of stationary points to be estimated. The stabilities of the various structures were expressed on the enthalpy scale. The enthalpy H resulted from correcting the electronic energy E for zero-point vibration terms, thermal contributions to energy from vibrations, rotations, and translations, and the pV terms. For estimating B3LYP and MP2 enthalpies, the B3LYP and MP2 electronic energies were supplemented with zero-point energy, and thermal contributions were calculated at the same B3LYP/6-311G(d,p) level. The values of H (discussed below) were obtained for $T = 298$ K and $p = 1$ atm in the harmonic oscillator–rigid rotor approximation.

The theoretical estimates of dissociation ($\Delta_d H^\circ$) and activation ($\Delta_a H^\circ$) enthalpies were derived from the calculated crystal lattice energies and DFT, MP2, and G2 gas-phase stabilities of NEt_4^+ and halogen ions X^- , decomposition products, triethylamine (NEt_3), and haloethane (EtX) and the respective transition state geometries. Thus, $\Delta_d H^\circ$ was calculated as the sum of the lattice energy and the energy released when isolated ions are transformed into dissociation products ($\text{NEt}_4^+_{(g)} + \text{X}^-_{(g)} \rightarrow \text{NEt}_3_{(g)} + \text{EtX}_{(g)}$). On the other hand, $\Delta_a H^\circ$ was computed as the sum of the energy required to form a gas phase ion conglomerate (van der Waals complex) and the activation enthalpy for the decomposition process.

The gaseous products evolved in the course of decomposition were monitored by FTIR, and the IR spectra were compared to those predicted at the B3LYP level. The harmonic vibrational frequencies determined with the B3LYP method were usually of high quality.⁴⁴ The errors, determined through comparison with the experimental data, were systematic in nature, and a “scaling factor” was frequently used to correct for any remaining discrepancies. Here, two scaling factors were applied that had successfully been used in the past to interpret IR spectra of gaseous arginine.⁴⁴ Thus, a value of 0.9813 was adopted for frequencies < 2000 cm^{-1} , and the value of 0.9613, recommended by Wong,⁴⁵ was used for higher frequency modes. To facilitate comparison between the theoretical and experimental spectra, the theoretical spectra are also presented as a linear combination of Gaussian functions located at the positions defined by the calculated frequencies, the integrals of which are equal to the theoretical integrated infrared intensities. The widths of these Gaussians were obtained by the least-squares procedure to obtain the best fit to the experimental spectra.

Crystal lattice energies were calculated using the GULP program.⁴⁶ All quantum-chemical calculations were carried out with the MOPAC2000⁴⁷ and Gaussian 98⁴⁸ codes on a cluster of 32 bit Xeon/SCI Dolphin processors and a cluster of 2 × Pentium III processors.

3. Results and Discussion

3.1. Thermal Decomposition. Figure 1 shows the thermogravimetric traces recorded for the three halides under study.

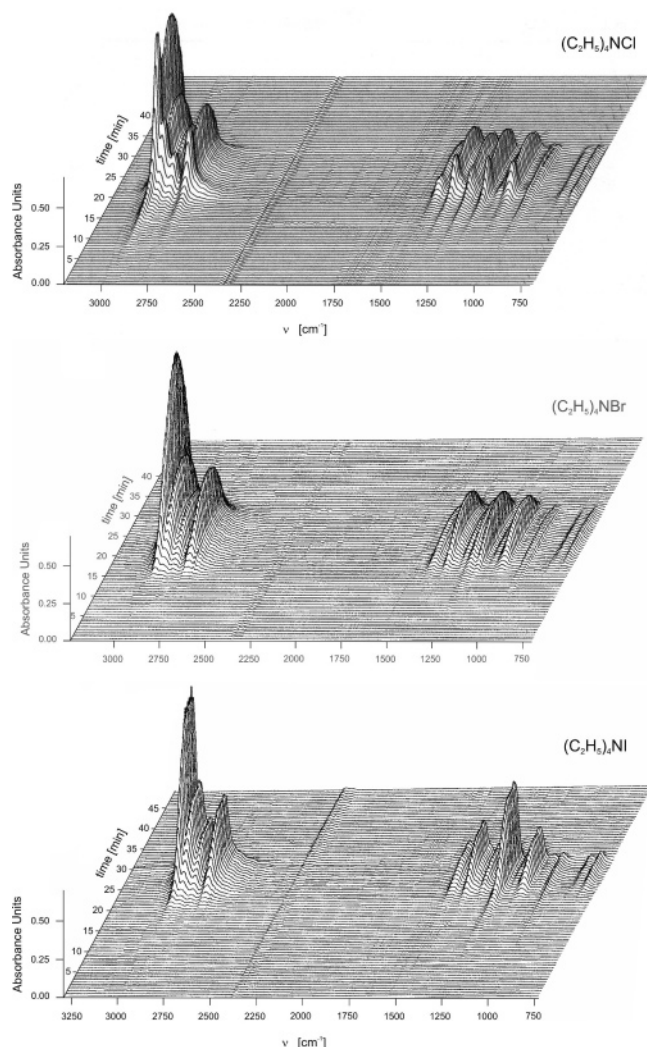
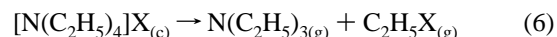


Figure 2. Time dependence of IR spectra measured during TG-FTIR experiments: tetraethylammonium chloride, tetraethylammonium bromide, and tetraethylammonium iodide.

The smooth shape of these TG curves suggests a simple one-step decomposition. The temperature for the onset of volatilization (490 K) was lowest for tetraethylammonium chloride (1) and highest (510 K) for tetraethylammonium iodide (3). In similar vein, tetraethylammonium chloride undergoes complete volatilization at 540 K but tetraethylammonium iodide undergoes complete volatilization at 545 K (see Figure 1).

The progress of volatilization was also monitored in that the IR spectra were recorded as a function of time (see Figure 2). The “three-dimensional” IR spectrum of tetraethylammonium chloride (see Figure 2) demonstrates that the intensities of the absorption signals pass through two successive maxima, an indication of the complex kinetics of this compound’s thermal decomposition. This is also reflected in the TG curve for tetraethylammonium chloride, which exhibits two inflection points (see Figure 1); these could be due to the exceptionally high hygroscopicity of the chloride. On the other hand, all the IR absorption bands of the three halides display the same pattern (see Figure 2), which suggests that the relevant products are formed at the onset of decomposition and at the end of this process.

It has long been suggested that quaternary ethylammonium halides dissociate with the release of triethylamine and the corresponding haloethanes. Hence, the proposed dissociation process can be described by the following equation:

where X stands for Cl, Br, or I. It should, however, be emphasized that the evidence confirming this mechanism is weak.¹⁵ Only recently, we pointed out that IR measurements combined with thermogravimetric experiments is a reliable method permitting the unambiguous identification of the species produced as a result of the thermal degradation of quaternary ethylammonium halides.²⁹ Here, to verify the validity of eq 6, we calculated the B3LYP frequencies of NEt_3 and of the respective EtX compounds and compared them with the IR spectra of the products formed during particular TG experiments. The harmonic frequencies, integrated intensities, symmetries, and description of the character of the IR modes, together with the experimental transition energies, are set out in Table S1 (see Supporting Information). Both NEt_3 and EtX compounds possess C_s symmetry, and therefore only transitions of a' and a'' symmetry appear in their IR spectra. The short wavelength region, above 2700 cm^{-1} , is dominated by strong NEt_3 stretching vibrations at 2797 and 2974 cm^{-1} of ca. 153 and 95 Km/mol , respectively (see Table S1). Medium-strength transitions due to NEt_3 are located above 2900 cm^{-1} , specifically at 2927 , 2980 , and 2982 of ca. 48, 64, and 45 Km/mol , respectively (see Table S1). In the low-frequency region, below 1500 cm^{-1} , crucial bands come from both species. For instance, medium-strength bending ($C-C-H$) transitions at 1071 , 1220 , 1377 , and 1380 cm^{-1} of ca. 25, 28, 24, and 27 Km/mol , respectively, are due to Et_3N absorption, whereas those at 1299 , 1255 , and 1221 cm^{-1} of ca. 43, 62, and 90 Km/mol originate from C_2H_5Cl , C_2H_5Br , and C_2H_5I , respectively (Table S1). Haloethanes also exhibit medium-absorption bands related to $C-H$ stretching above 2900 cm^{-1} , which overlap the NEt_3 bands, as well as characteristic transitions below 700 cm^{-1} due to the $C-X$ stretching mode (see Table S1).

Figure 3 illustrates the calculated and experimental IR spectra. On the basis of eq 6, we assumed an equimolar mixture of gaseous products and marked the theoretical transitions with bars of a height proportional to the calculated intensity, scaled accordingly (see Figure 3). Furthermore, to facilitate the comparison between the theoretical and experimental results, we expressed the calculated spectra as a linear combination of Gaussian functions defined such that their integrals were equal to the calculated IR intensity. The widths of particular Gaussians were fitted, using the least-squares procedure, to reproduce the experimental picture. The very good accordance between the experimental and calculated spectra (see Figure 3) may be considered strong proof of the validity of eq 6.

3.2. Thermodynamics of Thermal Decomposition. Unlike the hydrohalides of various amines, quaternary salts reveal considerable discrepancies between the enthalpies of volatilization estimated from the thermodynamic cycle and those calculated on the basis of eq 1.^{13–15} The DSC volatilization values for tetraethylammonium bromide and iodide are visibly smaller, whereas that for tetraethylammonium chloride is larger than the figures resulting from eq 1 (see Table 1). It should, of course, be realized that, unlike the DSC values of thermodynamic barriers, $\Delta_d H^\circ$ values resulting from the fitting to TG traces do not refer to 298 K.¹³ One should also emphasize here that the enthalpy of dissociation obtained with the aid of DSC can be considered the most accurate figure, since DSC is a direct technique, not requiring any fitting procedure or the use of a thermodynamic cycle.

As stated in the Introduction, the long-term goal of studying the decomposition of solids is to develop a theory based on

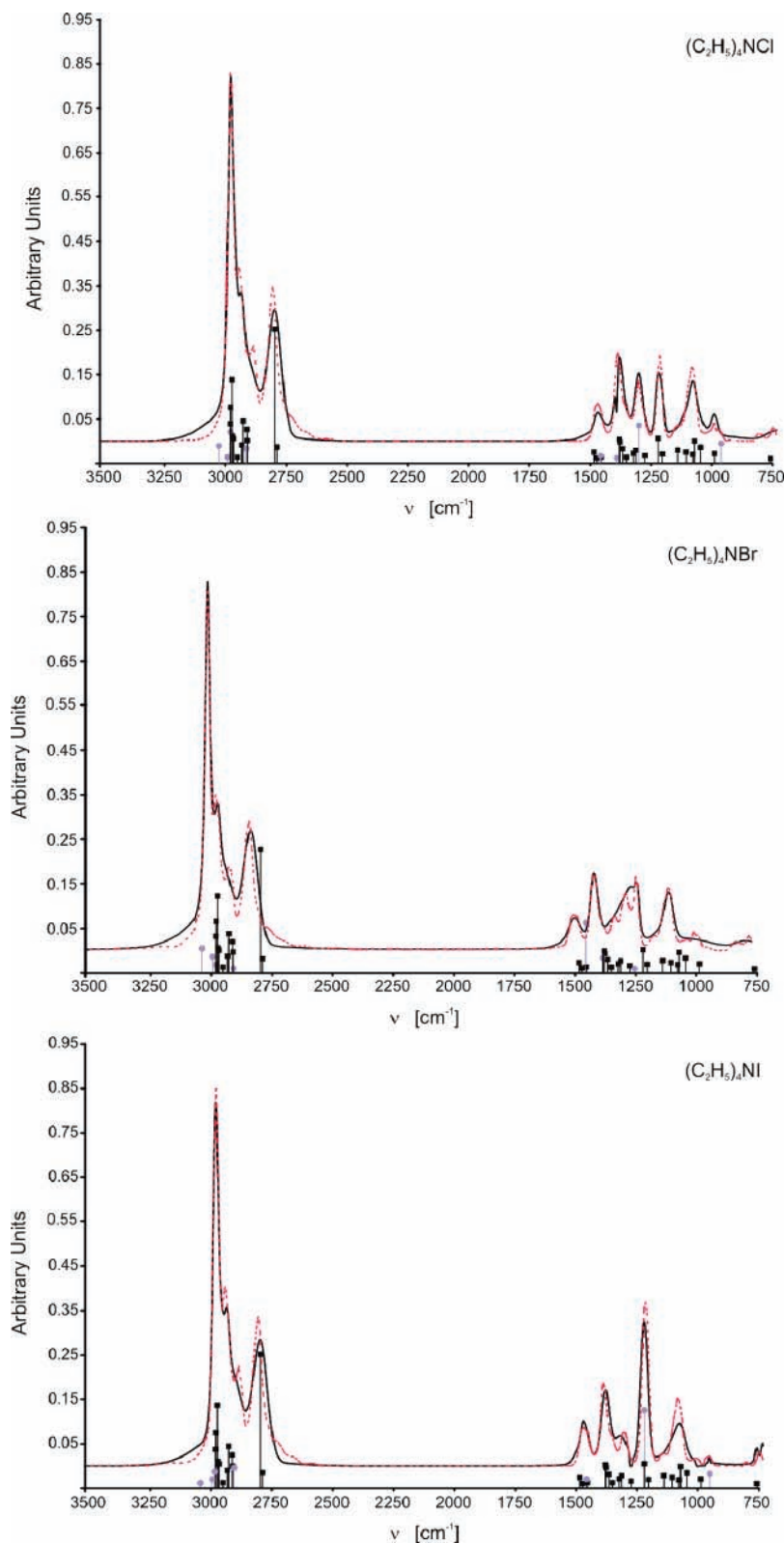


Figure 3. Comparison between experimental and theoretical IR spectra. Solid lines denote experimental spectra; dotted lines indicate the fit to the experimental spectrum with Gaussian functions (see Methods). The vertical bars refer to the calculated integrated intensities: squares, triethylamine; circles, ethyl halide.

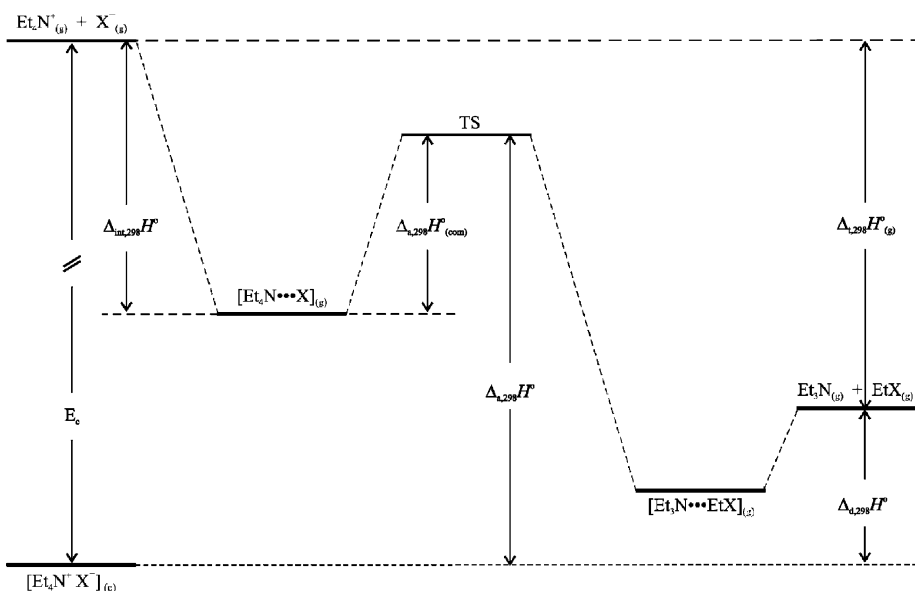
molecular-level data that explains their thermal stability and predicts their thermal behavior. In the following we shall demonstrate that an approach relying on a sufficiently accurate quantum-chemical treatment combined with crystal lattice energies is indeed able to predict the thermodynamic characteristics of thermal decay with acceptable accuracy.

Figure 4 depicts the thermodynamic cycle used to analyze theoretically the thermal decomposition of the title compounds. To reproduce the thermodynamic barrier to dissociation, we need to know the crystal lattice energy (E_c ; Figure 4), as well as the enthalpies of the isolated ions (${}_{298}H^\circ(\text{NET}_4^+)$ and ${}_{298}H^\circ(\text{X}^-)$; Figure 4) and those of the isolated products (${}_{298}H^\circ(\text{NET}_3)$ and

TABLE 1: Experimental and Theoretical Enthalpies of Dissociation ($\Delta_{\text{d},298}H^\circ$; $\text{Et}_4\text{NX}_{(\text{c})} \rightarrow \text{Et}_3\text{N}_{(\text{g})} + \text{EtX}_{(\text{g})}$) and Enthalpies of the Conversion of Ions in Isolation into Products in Isolation ($\Delta_{\text{t},298}H^\circ$; $\text{Et}_4\text{N}^+_{(\text{g})} + \text{X}^-_{(\text{g})} \rightarrow \text{Et}_3\text{N}_{(\text{g})} + \text{EtX}_{(\text{g})}$) Together with Total Crystal Lattice Energies (E_{c}) and Their Electrostatic Contribution (E_{e})

compound	$\Delta_{\text{d},298}H^\circ$						$\Delta_{\text{t},298}H^\circ$			crystal energy	
	experimental			theoretical ^c			B3LYP	MPW1K	MP2	E_{el}	E_{c}
	DSC	TG ^b	TG	B3LYP	MPW1K	MP2					
$[\text{N}(\text{C}_2\text{H}_5)_4]\text{Cl}$	158.4 ± 1.2	123.3 ± 4.6	196^{13}	159.5	172.5	170.3	405.0	392.9	395.0	476.8	565.3
$[\text{N}(\text{C}_2\text{H}_5)_4]\text{Br}$	181.1 ± 6.5	191.9 ± 3.5	405^{14}	144.9	165.5	168.9	393.0	372.4	368.9	459.0	537.8
$[\text{N}(\text{C}_2\text{H}_5)_4]\text{I}$	195.4 ± 8.9	229.1 ± 7.9	502^{15}	190.9	214.6	221.3	348.8	325.1	318.4	464.6	539.7

^a All values in kJ/mol. ^b From the least-squares fit of eq 1 to a thermogravimetric trace. ^c All values were estimated using the electronic energies of ions in isolation and decomposition products calculated at the level indicated in the column heading; zero-point energies and thermal contributions to enthalpy were obtained at the B3LYP/6-311G(d,p) level.

**Figure 4.** Thermodynamic cycle depicting the decomposition process.**TABLE 2: Experimental and Theoretical Enthalpies of Activation ($\Delta_{\text{a},298}H^\circ$; $[\text{Et}_4\text{N}^+\text{X}^-]_{(\text{c})} \rightarrow \text{Et}_3\text{N}_{(\text{g})} + \text{EtX}_{(\text{g})}$) for the Thermal Decomposition of Quaternary Ethylammonium Halides^a**

compound	experimental TG ^b	theoretical		
		B3LYP	MPW1K	MP2
$[\text{N}(\text{C}_2\text{H}_5)_4]\text{Cl}$	184.3 ± 13.1	285.7	307.9	298.1
$[\text{N}(\text{C}_2\text{H}_5)_4]\text{Br}$	285.8 ± 7.4	262.2	287.8	278.8
$[\text{N}(\text{C}_2\text{H}_5)_4]\text{I}$	386.9 ± 2.8	294.8	320.3	314.8

^a All values in kJ/mol. ^b From the least-squares fit of eq 2 to a thermogravimetric trace.

$_{298}H^\circ(\text{EtX})$; see Figure 4). In our previous reports on the lattice energy of the salts of organic bases, we suggested that the electrostatic contribution to the crystal lattice energy should alone account for the cohesive forces with commendable accuracy, since the repulsion and dispersion terms (see eq 3) cancel each other out. To test this assumption, we calculated both the electrostatic energy and the total lattice energy of the compounds under investigation. We modeled the sum of the repulsion and dispersion terms by employing the Filippini and Gavezotti³⁴ as well as the Goddard et al.³⁵ parameters. The former set was obtained by using as reference data the distribution of interatomic distances in 1846 organic crystals, the heats of sublimation of 122 compounds, and the structural data for 217 crystals.³⁴ On the other hand, Goddard et al. tested their parameters against 76 accurately determined crystal structures of organic compounds, the rotational barriers of a number of molecules, and the relative conformational energies and barriers of many molecules.³⁵ We can therefore regard these intermolecular potentials as extremely accurate.

Analysis of the data in Table 1 indicates that the assumption of the negligible value of the sum of repulsion and dispersion

terms does not hold for the quaternary salts we have analyzed. If we compare the figures in the last two columns of Table 1, we shall see that the total crystal lattice energy is larger than its electrostatic part by ca. 75–90 kJ/mol, which accounts for as much as 14–17% of the total effect. Therefore, when predicting the thermal stability of solids, even of ionic ones, we recommend using the total crystal energy instead of limiting the analysis to the electrostatic part of the cohesive forces.

Table 1 shows three quantum-chemical estimates of the enthalpy of decomposition. These barriers are the result of employing the following equation (cf. Figure 4):

$$\Delta_{\text{d},298}H^\circ = E_{\text{c}} + \{ \{_{298}H^\circ(\text{NEt}_3_{(\text{g})}) + _{298}H^\circ(\text{EtX}_{(\text{g})}) \} - \{ _{298}H^\circ(\text{NEt}_4^+_{(\text{g})}) + _{298}H^\circ(\text{X}^-_{(\text{g})}) \} \} \quad (7)$$

where E_{c} is the crystal lattice energy; $_{298}H^\circ(\text{species})$ represents the quantum-chemical enthalpies derived for the reactants in the gaseous phase (species = NEt_4^+ , X^- , NEt_3 , or EtX). These barriers agree quite well with the experimental DSC results (see Table 1). The greatest deviation (19.9%) is observed at the

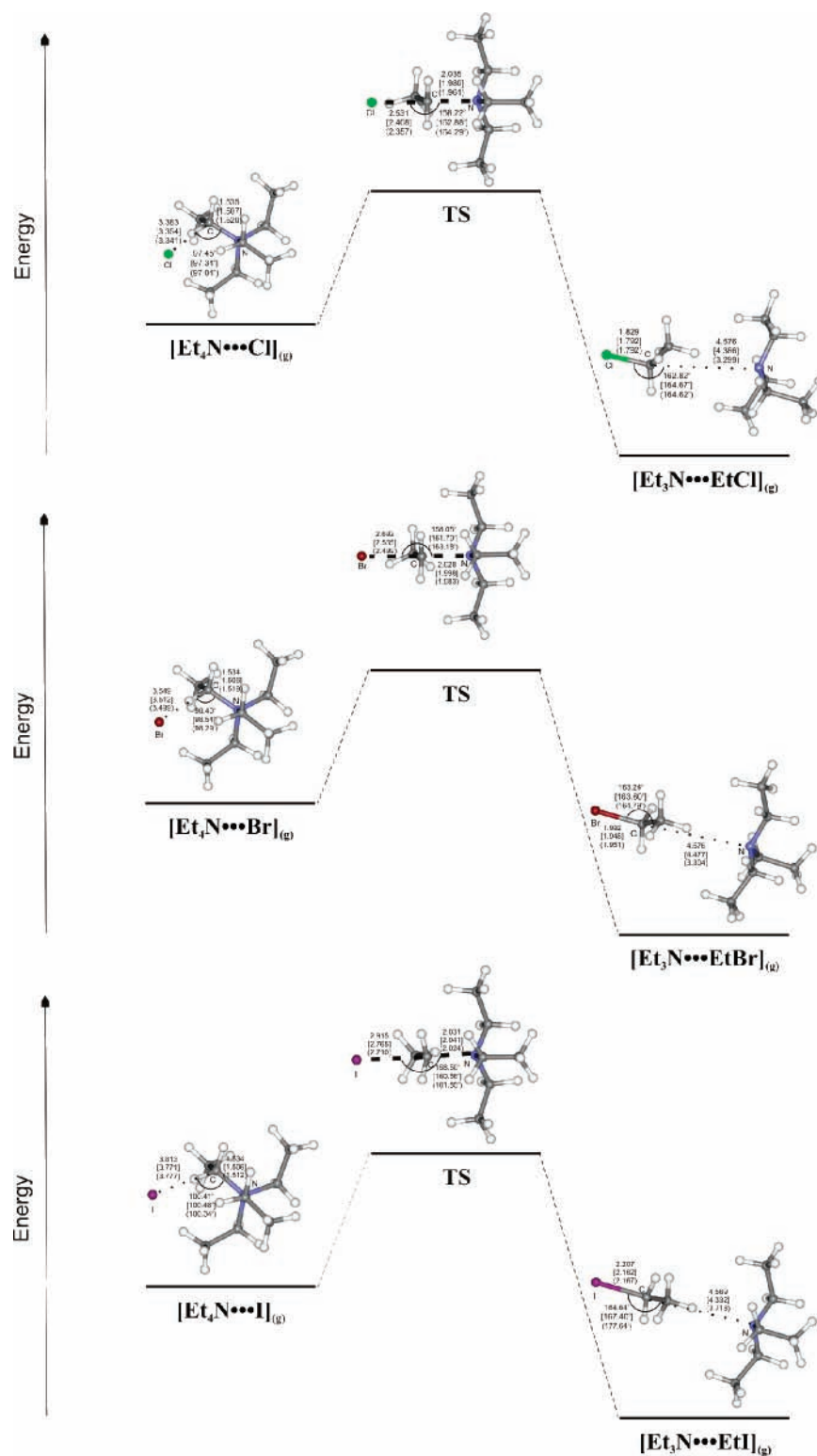


Figure 5. Geometries of stationary points for the gas-phase decomposition process calculated at the B3LYP (without brackets), MPW1K (square brackets), and MP2 (parentheses) levels.

B3LYP level for tetraethylammonium iodide and the smallest one (0.7%) is observed for tetraethylammonium chloride, also calculated with the B3LYP method. Hence we can conclude that the approach we propose in this paper makes a reasonable assessment of the thermodynamic stability of quaternary salts.

Analysis of the data in Table 1 suggests that the best thermodynamic barriers (i.e., those most resembling the DSC enthalpies) are obtained at the B3LYP level. From the theoretical point of view, however, this finding is unjustified, since MP2

and MPW1K usually work better than B3LYP. Indeed, on comparing the values of the second term on the right-hand side of eq 7, we find there are significant differences among the estimates obtained using the various methods. The B3LYP value is larger by ca. 30 kJ/mol than the MP2 estimate for $[\text{N}(\text{C}_2\text{H}_5)_4]\text{I}$, and by ca. 24 kJ/mol than the MPW1K prediction for $[\text{N}(\text{C}_2\text{H}_5)_4]\text{I}$. Therefore, taking into account the actual accuracy of the theoretical approaches we have employed in this work, we would expect the MP2/MPW1K assessment rather than the

TABLE 3: Interaction Energies^a in Ionic Pairs ($\Delta_{\text{int},298}H^\circ$; $\text{Et}_4\text{N}^+_{(\text{g})} + \text{X}^-_{(\text{g})} \rightarrow [\text{Et}_4\text{N}\cdots\text{X}]_{(\text{g})}$) and Activation Enthalpies for the Conversion of the Ionic Pair into Reaction Products ($\Delta_{\text{a},298}H^\circ_{(\text{com})}$; $[\text{Et}_4\text{N}\cdots\text{X}]_{(\text{g})} \rightarrow \text{Et}_3\text{N}_{(\text{g})} + \text{EtX}_{(\text{g})}$) Calculated at the B3LYP, MPW1K, and MP2 Levels^b

compound	$\Delta_{\text{int},298}H^\circ$			$\Delta_{\text{a},298}H^\circ_{(\text{com})}$		
	B3LYP	MPW1K	MP2	B3LYP	MPW1K	MP2
$[\text{N}(\text{C}_2\text{H}_5)_4]\text{Cl}$	353.2	357.7	366.5	73.6	100.6	99.2
$[\text{N}(\text{C}_2\text{H}_5)_4]\text{Br}$	347.5	350.7	361.8	71.9	100.3	102.7
$[\text{N}(\text{C}_2\text{H}_5)_4]\text{I}$	317.1	322.5	333.1	72.2	103.2	108.2

^a Uncorrected for BSSE; see Methods. ^b All values in kJ/mol.

B3LYP estimates to be most closely comparable to the DSC data. We can probably attribute these less-than-accurate predictions to the methods used for estimating the crystal lattice energy.

3.3. Kinetics of Thermal Decomposition. Table 2 compares the kinetic characteristics estimated from the kinetic model of volatilization (see eq 2) and from the combination of crystal lattice energies with the calculated quantum-chemical activation barriers (see Figure 4).

Three kinetic models — R1, R2, and F1 — were tested against the experimental data (α vs T ; see Figure 1). Earlier, the R1 (zero kinetic order) and R2 (surface contracting area) models had provided an adequate description of the thermal decomposition of halogen halides of organic amines, and the F1 model (unimolecular reaction) had best fitted the TG traces obtained for quaternary ethylammonium chloride.¹³ Using the least-squares procedure, we derived the activation energies for these three mechanisms; we always found the highest correlation coefficient for the F1 model. Table 2 shows the respective activation barriers. As the standard deviations indicate (see Table 2), the values for bromide and iodide were the most reliable; this may be explained by the fact that chloride is the most hygroscopic substance among the quaternary salts we investigated. In this context we may also recall the somewhat different behavior of the “three-dimensional” FTIR characteristic recorded for tetraethylammonium chloride and the other systems.

Since the unimolecular mechanism turned out to be the most appropriate for describing the experimental data, we also assumed in our theoretical model that decomposition proceeds in single-step fashion, via the same transition state that was localized for the gas-phase reaction involving the van der Waals (vdW) complex formed between the tetraethylammonium cation and the halogen anion $[\text{NEt}_4\cdots\text{X}]$. Figure 5 illustrates the structures of the stationary points. Transition state geometries suggest that the reaction proceeds by way of the well-known $\text{S}_{\text{N}}2$ mechanism. The $-\text{CH}_2\text{C}-$ fragment becomes planar, and the halogen atom and triethylamine are located at the opposite sides of the plane defined by $-\text{CH}_2\text{C}-$ (see Figure 5). As indicated by the geometric parameters, all the methods predict very similar geometries for the ion pair, transition state, and product complex: the lengths of the corresponding covalent bonds differ by less than 0.03 Å and those of the transition state bonds by less than 0.2 Å (see Figure 5). However, as far as the energetics are concerned, the situation appears to be different. Table 3 sets out the quantum-chemical characteristics used to calculate the activation barriers. Here we notice significant differences between the barriers estimated with the B3LYP model and those calculated with other methods. For instance, the enthalpies of activation of these salts are on the order of 100 kJ/mol with the MP2 and MPW1K models, ca. 70 kJ/mol with B3LYP. DFT methods, including the B3LYP functional, are known to underestimate activation barriers in comparison with experimental values or with the results of accurate ab initio calculations.^{49–52} This effect becomes obvious

when we analyze the data in Table 3. It is worth stressing that the MPW1K functional recommended for transition state modeling, also one of the DFT methods, does not have this disadvantage (see Table 3). Our recommendation is therefore to use the efficient and accurate MPW1K model for calculating activation barriers. On the other hand, analysis of the values of the $\Delta_{\text{int},298}H^\circ$ term indicates that all theoretical methods yield a very similar magnitude of this characteristic. The absolute difference between the lowest estimate and the highest estimate of the interaction energy in ion pairs does not exceed 16 kJ/mol (cf. the $[\text{N}(\text{C}_2\text{H}_5)_4]\text{I}$ entries in Table 3).

As we stated earlier, we calculated the activation barrier for the overall decomposition ($\Delta_{\text{a},298}H^\circ$; Figure 4) as the sum of the energy required to form the vdW complex and the activation enthalpy for the $[\text{NEt}_4\cdots\text{X}]_{(\text{g})} \rightarrow \text{Et}_3\text{N}_{(\text{g})} + \text{EtX}_{(\text{g})}$ reaction (see Figure 4). The activation enthalpy estimated from the fit of the F1 kinetic model to thermogravimetric traces and that calculated in the manner described above agree reasonably well, irrespective of the level of theory used (see Table 3), which suggests that the assumed mechanism is indeed operative.

4. Conclusions

In this work we have studied the behavior of selected quaternary ethylammonium halides at elevated temperatures. We analyzed the thermal decomposition of the title compounds using the TG-FTIR and DSC experimental techniques as well as the DFT and MP2 quantum-chemical treatments.

The smooth shape of the TG curves suggests a simple one-step decomposition. This inference is confirmed by the time dependency of the IR spectra of the gaseous decomposition products. After an initial increase, the absorption signal passes through a maximum, and then decreases gradually. All the IR absorption bands behave in the same manner, suggesting that the relevant products are formed at the onset of decomposition and at the end of this process. The perfect accordance between the experimental IR spectra and those predicted at the B3LYP/6-311G(d,p) level demonstrates for the first time that the decomposition produces an equimolar mixture of triethylamine and the ethyl halide.

The good correlation between the calculated and measured enthalpies of dissociation indicates that the computational chemistry methods are a valuable tool enabling reliable predictions to be made about the thermal stability of solid materials. Comparison of the electrostatic contribution to the crystal lattice energy with the total E_{c} demonstrates the importance of the repulsion–dispersion term, which was frequently neglected in the past. The correspondence between the experimental and theoretical estimates of $\Delta_{\text{d},298}H^\circ$ was best at the B3LYP level, which, taking into account the quality of the theoretical models employed, we can attribute to inaccuracies in estimating the crystal lattice energy.

Of the three kinetic models used to fit the experimental data, the F1 unimolecular mechanism turned out to be the most relevant (for thermal decomposition proceeding on/in the crystal,

the R1 or R2 model should be more suitable). Employing the calculated crystal lattice energies in tandem with the quantum-chemical kinetic barriers estimated for a unimolecular decomposition, we were able to evaluate the theoretical activation energies. Like the thermodynamic characteristics, the activation energies are also best reproduced at the MPW1K level. Comparison of the activation barriers predicted with the three quantum-chemical methods shows that the B3LYP model significantly underestimates the kinetic barriers. The MPW1K functional seems to be the most appropriate substitute for the B3LYP.

In summary, we have demonstrated that theoretical methods can predict relevant characteristics of the thermal decomposition of solid materials with experimental accuracy. For the quantum-chemical description of thermal decomposition we recommend DFT methodologies, in particular the MPW1K functional for evaluating thermodynamic barriers and for assessing activation characteristics. These quantum-chemical data have to be combined with crystal lattice energies, which should be calculated using both the electrostatic and the repulsion–dispersion terms.

Despite the good agreement between our theoretical and experimental data, we would like to emphasize that a more elaborate theoretical model is needed to describe the overall thermal decomposition more precisely. For instance, in our theoretical model the ionic pair is first moved from the crystalline phase to the gaseous phase, and only then does it undergo a chemical conversion. This approach allows us to use standard procedures for TS localization. However, the chemical reaction might also begin while the ionic pair is still interacting with the crystal surface. Therefore, we plan to improve the present model by using a hybrid quantum-mechanical/quantum-mechanical method to localize the TS structure for the ionic pair interacting with the crystal. In this approach, the crystal surface in the immediate vicinity of the ionic pair will be modeled by several tetraethylammonium cations and halogen ions arranged in accordance with the experimental crystal structure and described at a lower level of theory than the ionic pair itself, while the remainder of the crystal will be represented by a set of point charges located at the crystal lattice nodes.

Acknowledgment. This work was supported by the Polish State Committee for Scientific Research (KBN), Grant DS/8221-4-0140-6. The calculations were performed at the Academic Computer Center in Gdańsk (TASK).

Supporting Information Available: Harmonic unscaled and scaled vibrational frequencies together with the available experimental frequencies and their intensities for the decomposition products of quaternary ethylammonium halides calculated at the B3LYP/6-311G(d,p) level. This material is available free of charge via the Internet at <http://pubs.acs.org>.

References and Notes

- Wilk, K. A.; Bieniecki, A.; Burczyk, B.; Sokółowski, A. *J. Am. Oil Chem. Soc.* **1994**, *71*, 81.
- Ortel, J. *Holtztechnologie* **1982**, *6*, 243.
- Śliwa, W. *N-substituted salts of pyridine and other relative compounds; synthesis, properties and usage*; WSP: Częstochowa, 1996.
- Reuter, G. *Med. Weter.* **1995**, *51*, 128.
- Starks, C. M.; Liotta, C. L.; Halpern M. *Phase-Transfer Catalysis Fundamentals, Applications and Industrial Perspectives*; Chapman and Hall: London, 1994.
- Carmichel, A. J.; Haddelton, D. M.; Bon, S.; Seddon, K. R. *Chem. Commun.* **2000**, 1237.
- Kabalka, G. W.; Malldi, R. R. *Chem. Commun.* **2000**, 2191.
- Song, E. C.; Roh, E. J. *Chem. Commun.* **2000**, 837.
- Earle, M. J.; McCormac, P. B.; Seddon, K. R. *Chem. Commun.* **1998**, 2245.
- Stenes, S.; Wasserschied, P.; Diessen-Hoelscher, B. *J. Prakt. Chem.* **2000**, *342*, 348.
- Song, C. E.; Shim, W. H.; Roh, E. J.; Choi, J. H. *Chem. Commun.* **2000**, 1965.
- Le Boulaire, V.; Gree, R. *Chem. Commun.* **2000**, 2195.
- Błażejowski, J.; Kowalewska, E. *Thermochim. Acta* **1986**, *105*, 257.
- Łubkowski, J.; Błażejowski, J. *Thermochim. Acta* **1990**, *157*, 259.
- Dokurno, P.; Łubkowski, J.; Błażejowski, J. *Thermochim. Acta* **1990**, *165*, 31.
- Galwey, A. K.; Brown, M. E. *Thermal Decomposition of Ionic Solids*; Elsevier: Amsterdam, 1999.
- Łubkowski, J.; Błażejowski, J. *J. Chem. Soc., Faraday Trans. 1* **1986**, *82*, 3069.
- Łubkowski, J.; Błażejowski, J. *Thermochim. Acta* **1987**, *121*, 413.
- Smith A.; Calvert, R. P. *J. Am. Chem. Soc.* **1914**, *26*, 1363.
- Perrier-Datin, A.; Julien-Laferriere, S.; Lebas, J. M.; Belloc, J. J. *Chim. Phys.* **1973**, *70*, 1684.
- Kapustinskii, A. F. *Q. Rev. (London)* **1956**, 283.
- Yatsmirski, K. B. *Zh. Neorg. Khim.* **1961**, *6*, 518.
- Łubkowski, J.; Błażejowski, J. *J. Therm. Anal.* **1990**, *36*, 2009.
- Łubkowski, J.; Dokurno, P.; Błażejowski, J. *Thermochim. Acta* **1991**, *176*, 183.
- Łubkowski, J.; Błażejowski, J. *J. Chem. Soc., Faraday Trans.* **1991**, *87*, 1333.
- Łubkowski, J.; Błażejowski, J. *J. Phys. Chem.* **1991**, *95*, 2311.
- Skurski, P.; Jasionowski, M.; Błażejowski, J. *J. Therm. Anal.* **1998**, *54*, 189.
- Ewald, P. P. *Ann. Phys. (Leipzig)* **1921**, *64*, 253.
- Błażejowski, J.; Krzymiński, K.; Storoniak, P.; Rak, J. *J. Thermal. Anal. Calorim.* **2000**, *60*, 927.
- Conway, B. E.; Verrall, R. E.; Desnoyers, J. E. *Trans. Faraday Soc.* **1966**, *62*, 2738.
- Sestak, J.; Satava, V.; Wendlandt, W. W. *Thermochim. Acta* **1973**, *7*, 333.
- Backingham, R. A. *Proc. Phys. Soc. (London)* **1938**, *A168*, 264.
- Besler, B. H.; Merz, K. M.; Kollman, P. A. *J. Comput. Chem.* **1990**, *11*, 431.
- Filippini, G.; Gavezzotti, A. *Acta Crystallogr., Sect. B* **1993**, *B49*, 868.
- Mayo, S. L.; Olafson, B. D.; Goddard III, W. A. *J. Phys. Chem.* **1990**, *94*, 8897.
- Staples, R. J. *Z. Kristallogr. New Cryst. Struct.* **1999**, *214*, 231.
- Ralle, M.; Bryan, J. C.; Habenschuss, A.; Wunderlich, B. *Acta Crystallogr., Sect. C: Cryst. Struct. Commun.* **1997**, *53*, 488.
- Vincent, B. R.; Knop, O.; Linden, A.; Cameron, T. S.; Robertson, K. N. *Can. J. Chem.* **1988**, *66*, 3060.
- Stewart, J. J. P. *J. Comput. Chem.* **1989**, *10*, 209; *J. Comput. Chem.* **1989**, *10*, 221.
- Becke, A. D. *Phys. Rev. A* **1988**, *38*, 3098. Becke, A. D. *J. Chem. Phys.* **1993**, *98*, 5648. Lee, C.; Yang, W.; Paar, R. G. *Phys. Rev. B* **1988**, *37*, 785.
- McLean, A. D.; Chandler, G. S. *J. Chem. Phys.* **1980**, *72*, 5639.
- Krishnan, R.; Binkley, J. S.; Seeger, R.; Pople, J. A. *J. Chem. Phys.* **1980**, *72*, 650.
- Lynch, B. J.; Fast, P. L.; Harris, M.; Truhlar, D. G. *J. Phys. Chem. A* **2000**, *104*, 21.
- Rak, J.; Skurski, P.; Simons, J.; Gutowski, M. *J. Am. Chem. Soc.* **2001**, *123*, 11695.
- Wong, M. W. *J. Chem. Phys.* **1996**, *100*, 391.
- Gale, J. D. *J. Chem. Soc., Faraday Trans.* **1997**, *93*, 629.
- Stewart, J. J. P. *MOPAC2000*; Fujitsu Limited: 1999.
- Frisch, M. J.; Trucks, G. W.; Schlegel, H. B.; Scuseria, G. E.; Robb, M. A.; Cheeseman, J. R.; Zakrzewski, V. G.; Montgomery, J. A., Jr.; Stratmann, R. E.; Burant, J. C.; Dapprich, S.; Millam, J. M.; Daniels, A. D.; Kudin, K. N.; Strain, M. C.; Farkas, O.; Tomasi, J.; Barone, V.; Cossi, M.; Cammi, R.; Mennucci, B.; Pomelli, C.; Adamo, C.; Clifford, S.; Ochterski, J.; Petersson, G. A.; Ayala, P. Y.; Cui, Q.; Morokuma, K.; Salvador, P.; Dannenberg, J. J.; Malick, D. K.; Rabuck, A. D.; Raghavachari, K.; Foresman, J. B.; Cioslowski, J.; Ortiz, J. V.; Baboul, A. G.; Stefanov, B. B.; Liu, G.; Liashenko, A.; Piskorz, P.; Komaromi, I.; Gomperts, R.; Martin, R. L.; Fox, D. J.; Keith, T.; Al-Laham, M. A.; Peng, C. Y.; Nanayakkara, A.; Challacombe, M.; Gill, P. M. W.; Johnson, B.; Chen, W.; Wong, M. W.; Andres, J. L.; Gonzalez, C.; Head-Gordon, M.; Replogle, E. S.; Pople, J. A. *Gaussian 98*, revision A.11; Gaussian, Inc.: Pittsburgh, PA, 2001.
- Sadhukhan, S.; Munoz, D.; Adamo, C.; Scuseria, G. E. *Chem. Phys. Lett.* **1999**, *306*, 83.
- Lynch, B. J.; Truhlar, D. G. *J. Phys. Chem. A* **2001**, *105*, 2936.
- Lynch, B. J.; Fast, P. L.; Harris, M.; Truhlar, D. G. *J. Phys. Chem. A* **2000**, *104*, 21.
- Jursic, B. S. *Theoretical and Computational Chemistry*; Elsevier: Amsterdam, 1996. Vol. 4.